

### 33. *Magnetic Anomaly over a Magnetized Circular Cone.*

By Tsuneji RIKITAKE and Yukio HAGIWARA,

Earthquake Research Institute.

(Read June 22, 1965.—Received June 23, 1965.)

#### Summary

A computer programme for studying magnetic anomaly over a magnetized circular cone is set out. A number of examples of anomaly are then computed and illustrated. These anomaly patterns would be of some use for interpreting aeromagnetic maps. It is pointed out on the basis of a two-cone model that topography effect should be carefully eliminated from an aeromagnetic map in order to say something about underground structure.

#### 1. Introduction

Aeromagnetic surveys over a number of Japanese volcanoes have been conducted as one of the projects of the U.S.-Japan Scientific Co-operation since 1963. These surveys provided aeromagnetic maps which are useful for studying underground structure of the volcanoes. Since many of these volcanoes are Quaternary ones composed of basaltic and andesitic rocks having fairly strong magnetizations, we often see on these aeromagnetic maps characteristic patterns of magnetic anomaly which is doubtlessly caused by the magnetization of mountain body, central cone, peak on caldera rim and the like. It appears to the writers, therefore, that it would be a nice thing to demonstrate typical anomalies over a magnetized circular cone which, in many cases, approximates very well the mountain body concerned.

Magnetic anomaly associated with a volcano has long been a topic in the study of geomagnetism. In order to interpret the anomaly revealed by a land magnetic survey, T. Minakami<sup>1)</sup> replaced a volcano by one or two rotational ellipsoids which were uniformly magnetized. T. Rikitake<sup>2)</sup> calculated anomalies produced by a uniformly magnetized circular cone.

1) T. MINKAMI, *Bull. Earthq. Res. Inst.*, **16** (1938), 100; **18** (1940), 178.

2) T. RIKITAKE, *Bull. Earthq. Res. Inst.*, **29** (1951), 161; **30** (1952), 71.

The main difficulty in these studies was the labour of numerical work. Such a difficulty has been removed, however, in recent years by the use of a high-speed computer. Even magnetic anomaly due to a magnetized body of arbitrary shape can be calculated without difficulty.<sup>3)</sup>

It is aimed at demonstrating in this paper typical anomalies over a circular cone on the basis of analytical formulas as previously obtained by one of the writers (T.R.).<sup>2)</sup> In Section 2, such formulas will be summarized. Several examples of anomalies will be illustrated in Section 3. The anomaly when two cones are closely placed with one another will be shown in Section 4 in the hope of getting some idea about an anomaly over rugged topography.

## 2. Magnetic field associated with a magnetized circular cone

Gravitational potential  $V$  of a circular cone having radius  $\alpha_0$  at the bottom and height  $h$  can be obtained by integrating that of circular disks. We obtain

$$V = 2\pi k^2 \sigma \int_z^h a dz_1 \int_0^\infty \frac{1}{\alpha} e^{-\alpha(z_1-z)} J_0(\alpha r) J_1(\alpha a) d\alpha \\ + 2\pi k^2 \sigma \int_0^z a dz_1 \int_0^\infty \frac{1}{\alpha} e^{-\alpha(z-z_1)} J_0(\alpha r) J_1(\alpha a) d\alpha \quad (1)$$

where  $k^2$ ,  $\sigma$  and  $r$  denote the gravitational constant, density and radial distance from the central axis ( $z$  axis) of the cone.  $J_0$  and  $J_1$  are Bessel functions.  $a$  is the radius of the cone at  $z=z_1$ . When the cone is uniformly magnetized in a direction with an inclination  $\theta$  in the  $xz$  plane, the magnetic field components due to the magnetization are easily calculated from Poisson's relations. The  $x'$ ,  $y'$  and  $z$  components are given by

$$\left. \begin{aligned} \Delta X' &= 2\pi J \left\{ \cos \theta \left( \frac{F}{r} \cos 2\phi - G \cos^2 \phi \right) - H \sin \theta \cos \phi \right\}, \\ \Delta Y' &= 2\pi J \left\{ \cos \theta \sin 2\phi \left( \frac{F}{r} - \frac{G}{2} \right) - H \sin \theta \sin \phi \right\}, \\ \Delta Z &= 2\pi J (G \sin \theta - H \cos \theta \cos \phi), \end{aligned} \right\} \quad (2)$$

where  $J$  is the intensity of magnetization and  $\phi$  the azimuthal angle of

3) e. g. V. VACQUIER, *Proc. Benedum Earth Magnetism Symp.*, (1962), 123.

a cylindrical coordinate of which the centre is taken at the centre of the bottom plane.  $\phi=0$  specifies the plane in which the  $x'$  axis lies.

$F, G$  and  $H$  in (2) are given by

$$\left. \begin{aligned} F &= \int_z^h aI_1 dz_1 + \int_0^z aI_1' dz_1, \\ G &= \int_z^h aI_2 dz_1 + \int_0^z aI_2' dz_1, \\ H &= \int_z^h aI_3 dz_1 - \int_0^z aI_3' dz_1, \end{aligned} \right\} \quad (3)$$

where

$$\left. \begin{aligned} \frac{I_1}{I_1'} &= \int_0^\infty e^{\mp\alpha(z_1-z)} J_1(\alpha a) d\alpha, \\ \frac{I_2}{I_2'} &= \int_0^\infty \alpha e^{\mp\alpha(z_1-z)} J_0(\alpha r) J_1(\alpha a) d\alpha, \\ \frac{I_3}{I_3'} &= \int_0^\infty \alpha e^{\mp\alpha(z_1-z)} J_1(\alpha r) J_1(\alpha a) d\alpha. \end{aligned} \right\} \quad (4)$$

For the convenience of numerical work,  $F, G$  and  $H$  are transformed to

$$\left. \begin{aligned} 2\pi F &= 2\alpha_0 \rho^{-1/2} \int_0^{h/a_0} \alpha^{1/2} \left( \frac{2-\kappa^2}{\kappa} K - \frac{2}{\kappa} E \right) d\zeta_1, \\ 2\pi G &= \rho^{-1/2} \int_0^{h/a_0} \kappa \alpha^{-1/2} \left\{ K + \frac{\kappa^2 \alpha / \rho - (2-\kappa^2)}{2(1-\kappa^2)} E \right\} d\zeta_1, \\ 2\pi H &= \rho^{-3/2} \int_0^{h/a_0} \kappa \alpha^{-1/2} (\zeta - \zeta_1) \left\{ -K + \frac{2-\kappa^2}{2(1-\kappa^2)} E \right\} d\zeta_1, \end{aligned} \right\} \quad (5)$$

in which

$$\left. \begin{aligned} \kappa^2 &= 4\alpha\rho / \{(\alpha + \rho)^2 + (\zeta - \zeta_1)^2\}, \\ a/a_0 &= \alpha, \quad r/a_0 = \rho, \quad z_1/a_0 = \zeta_1, \quad z/a_0 = \zeta, \end{aligned} \right\} \quad (6)$$

while  $K$  and  $E$  are the complete elliptic integrals.

A programme for computing  $\Delta X', \Delta Y'$  and  $\Delta Z$  at various heights was set out with appropriate function subprogrammes for  $E$  and  $K$ . The direction of the magnetization and the shape of the cone were taken into account as parameters.

Special caution should be paid to the calculation of the field components at points on the central axis because it is difficult to calculate

$F$ ,  $G$  and  $H$  directly from (5). Going back to (4), however, we see that the following holds good for  $r=0$  and  $z=h+d$ ;

$$\left. \begin{aligned} \frac{2F}{r} = G = \int_0^h \frac{(a_0 - kz_1)^2}{\{(a_0 - kz_1)^2 + (h + d - z_1)^2\}^{3/2}} dz_1, \\ H = 0, \end{aligned} \right\} \quad (7)$$

where

$$k = \cot \lambda, \quad (8)$$

while  $\lambda$  denotes the slope angle of the cone.

Performing the integration, we obtain

$$\begin{aligned} G = \frac{m}{(m^2 + 1)^{3/2}} \log \frac{\gamma + m\beta + m^2 + 1 + \sqrt{m^2 + 1} \sqrt{(1 + \gamma)^2 + (m + \beta)^2}}{\gamma + m\beta + \sqrt{m^2 + 1} \sqrt{\beta^2 + \gamma^2}} \\ + \frac{m}{m^2 + 1} \left\{ \frac{m^2 - 1 - (\gamma - m\beta)}{\sqrt{(1 + \gamma)^2 + (m + \beta)^2}} + \frac{\gamma - m\beta}{\sqrt{\beta^2 + \gamma^2}} \right\}, \end{aligned} \quad (9)$$

where

$$m = 1/k, \quad \beta = dm/h, \quad \gamma = c_0 m/h, \quad (10)$$

while  $c_0$  represents the radius of the top plane of the cone.

With  $G$  thus obtained, the field components at points on the central axis are given as

$$\left. \begin{aligned} \Delta X' &= -\pi JG \cos \theta, \\ \Delta Y' &= 0 \\ \Delta Z &= 2\pi JG \sin \theta. \end{aligned} \right\} \quad (11)$$

Since the field components  $\Delta X'$ ,  $\Delta Y'$ , and  $\Delta Z$  have been obtained in the above, the anomaly in the geomagnetic field referring to the geographic directions can easily be calculated. When the angle between the direction of magnetization and the  $x$  axis (northward) is designated by  $\psi$  as can be seen in Fig. 1, the anomalies in the  $x$  and  $y$  components are obtained as

$$\left. \begin{aligned} \Delta X &= \Delta X' \cos \psi - \Delta Y' \sin \psi, \\ \Delta Y &= \Delta X' \sin \psi + \Delta Y' \cos \psi. \end{aligned} \right\} \quad (12)$$

If we assume that  $\Delta X$ ,  $\Delta Y$  and  $\Delta Z$  are much smaller than the absolute

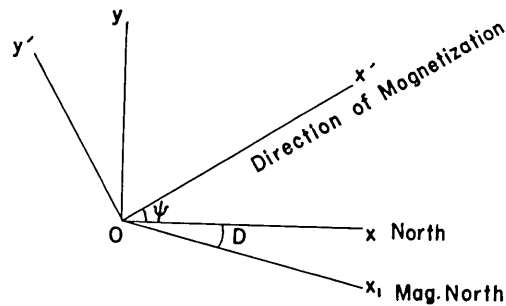


Fig. 1. Coordinate systems

values of the present geomagnetic field, the anomaly in the total intensity is given by

$$\Delta F = (\Delta X \cos D + \Delta X \sin D) \cos I + \Delta Z \sin I, \quad (13)$$

where  $D$  is the declination and  $I$  the inclination of the geomagnetic field. Taking  $\psi$ ,  $D$  and  $I$  as parameters, the anomaly for various magnetic elements can readily be computed.

### 3. Examples of anomaly

In order to demonstrate typical patterns of anomaly over relatively young volcanoes like Oshima Island,  $\Delta X$ ,  $\Delta Y$ ,  $\Delta Z$  and  $\Delta F$  at various heights over a circular cone of which the slope angle amounts to  $10^\circ$  and the ratio of the top radius  $c_0$  to the bottom radius  $a_0$  amounts to 0.1 are calculated. It is assumed that the direction of magnetization agrees with that of the geomagnetic field, so that  $\psi = 0$  and  $\theta = I$ . For the purpose of applying the cone to volcanoes in the central area of Japan,  $\theta = 48^\circ$  is assumed.  $D = 0$  is also assumed for the sake of simplicity.

Figs. 2, 3, 4 and 5 show the anomalies at heights 0.2, 0.3, 0.5 and 1.0 in units of the bottom radius  $a_0$ . Unit value is assumed for intensity of magnetization  $J$ . In the actual calculation all lengths are measured in units of  $a_0$ . Looking at the figure from Fig. 2 to Fig. 5, we see that the anomaly resembles that of a magnetic dipole dipping northwards. Such a fact has been well-recognized many years ago. It would nevertheless be useful to compare the anomaly pattern of total intensity to actual examples often found on an aeromagnetic map for obtaining some idea of the effect of a certain mountain body.

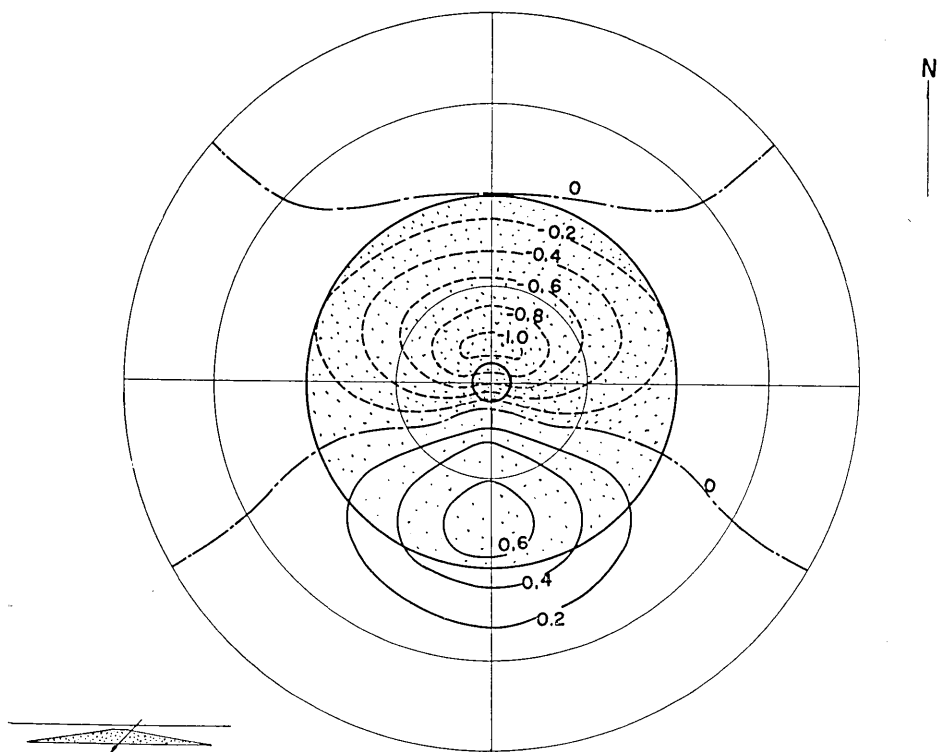


Fig. 2a.  $\Delta X$  over a magnetized circular cone, which is shown by the shaded circle, at a height of 0.2 in units of the bottom radius. The numerals indicate the field intensity when the intensity of magnetization and the bottom radius are taken as unity. It is assumed that the direction of magnetization lies in the magnetic meridian plane and that its inclination agrees with the geomagnetic dip which is taken as  $48^\circ$ . The slope angle is assumed as  $10^\circ$ .

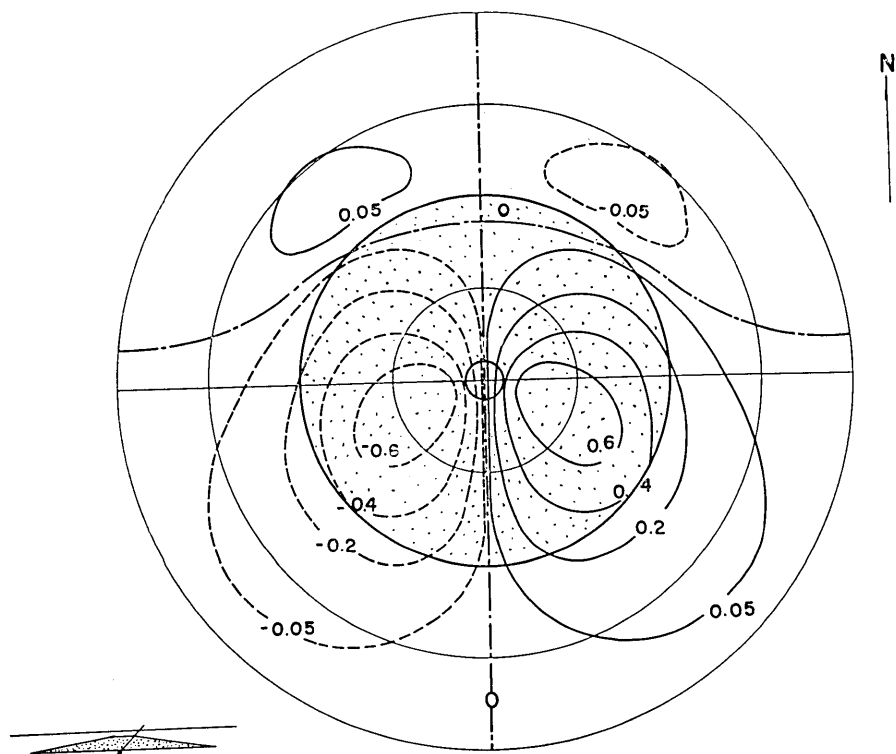


Fig. 2b.  $\Delta Y$  for the cone and the flight height as defined in the caption of Fig. 2a.

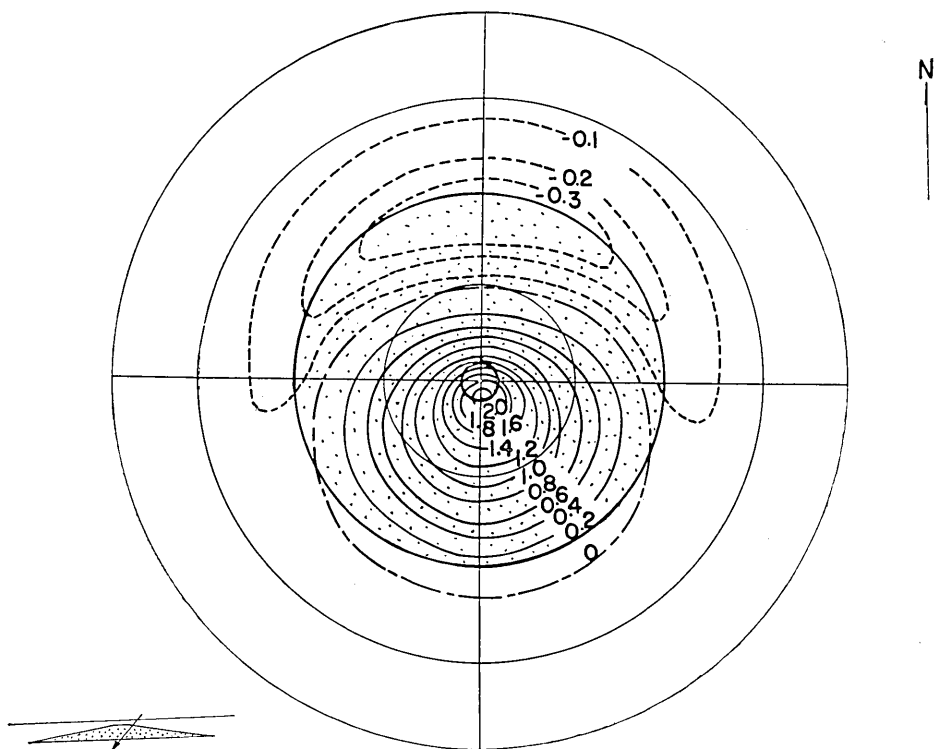


Fig. 2c.  $\Delta Z$  for the cone and the flight height as defined in the caption of Fig. 2a.

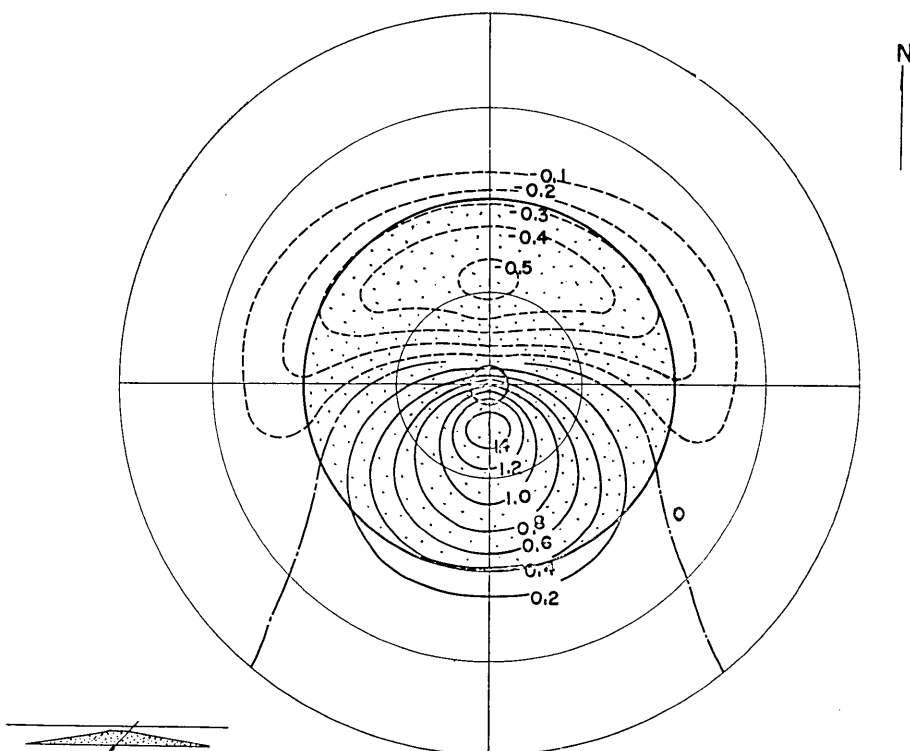


Fig. 2d.  $\Delta F$  for the cone and the flight height as defined in the caption of Fig. 2a.

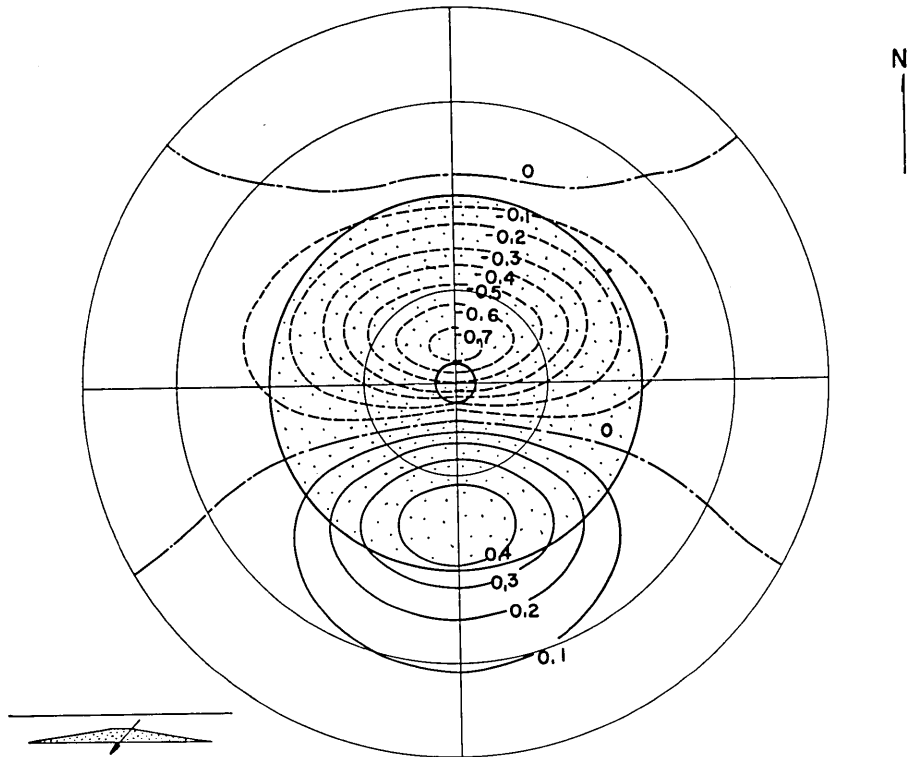


Fig. 3a.  $\Delta X$  over a cone of which all the parameters are the same as those for Fig. 2. The flight height is 0.3.

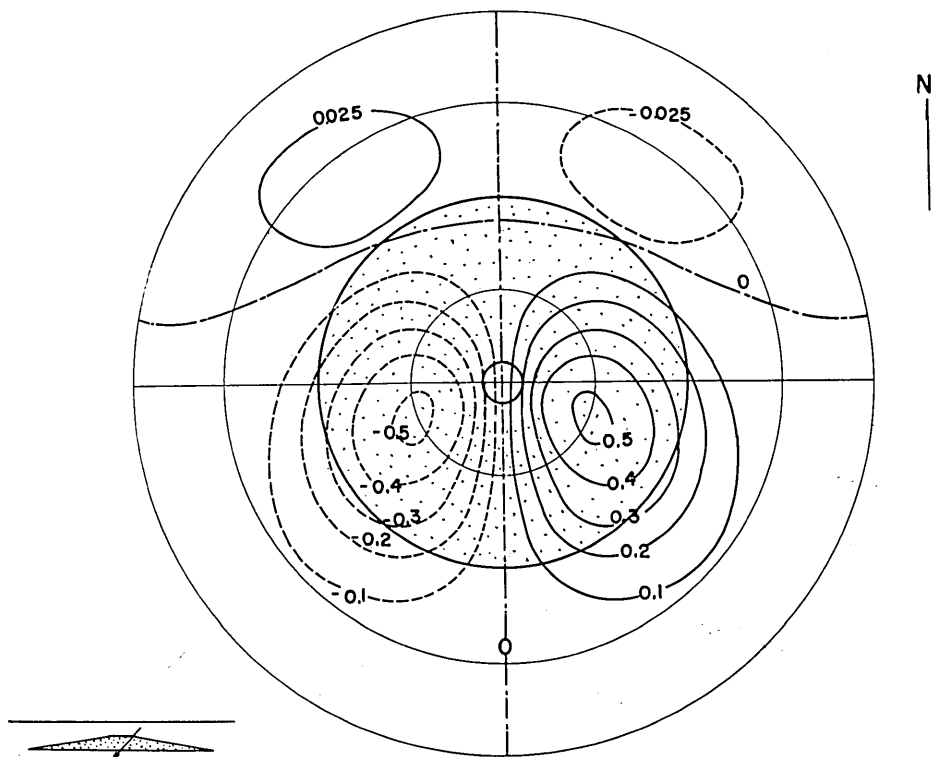


Fig. 3b.  $\Delta Y$  for the same conditions as those for Fig. 3a.

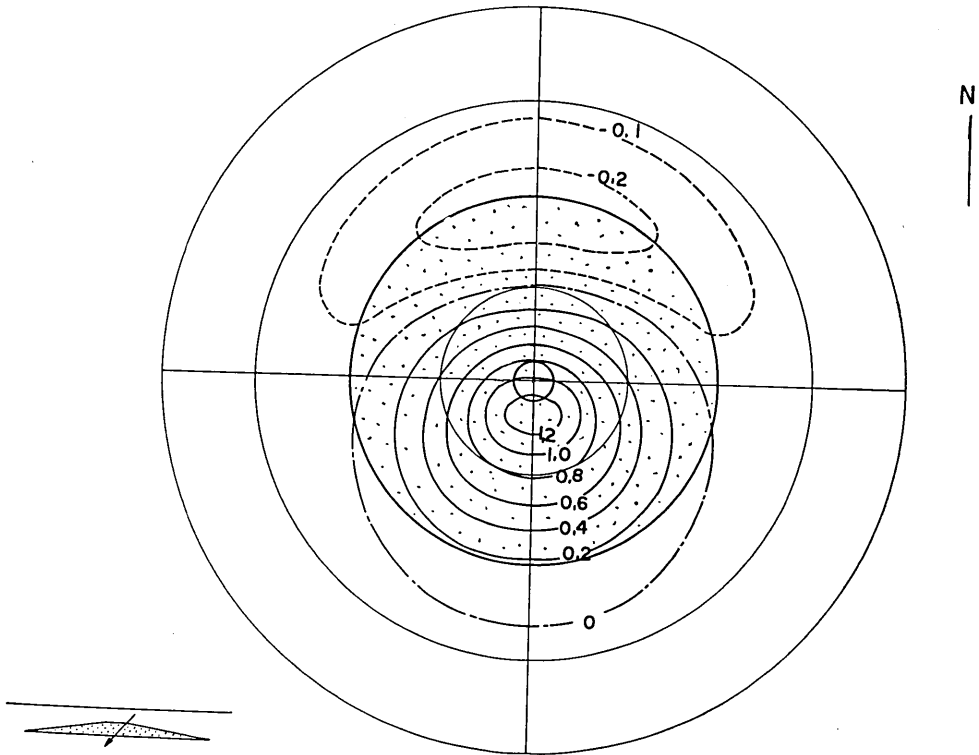


Fig. 3c.  $\Delta Z$  for the same conditions as those for Fig. 3a.

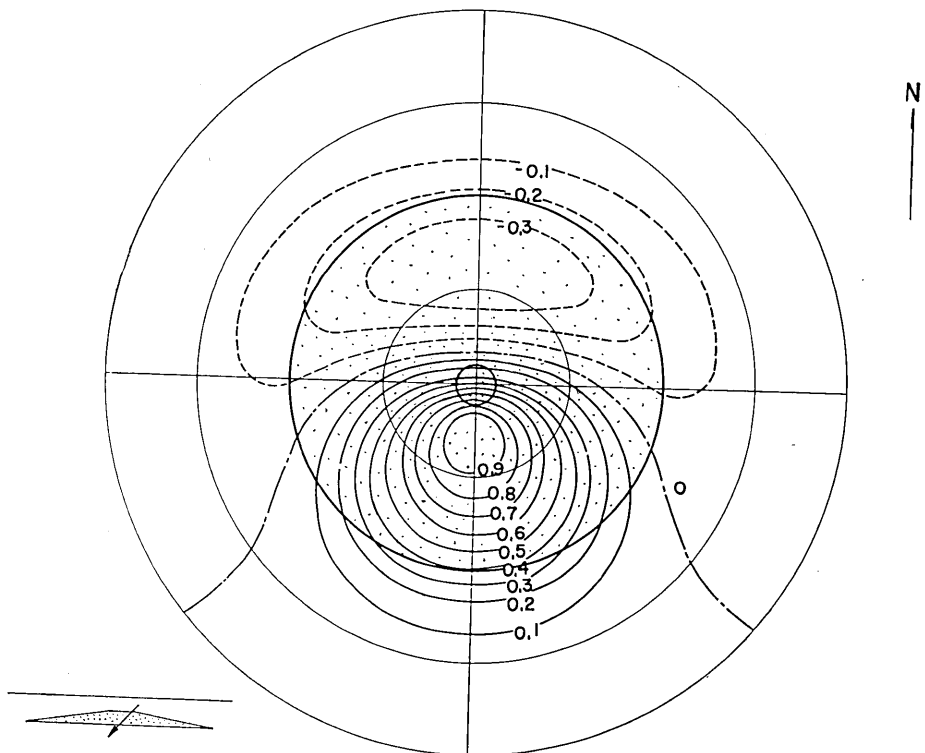


Fig. 3d.  $\Delta F$  for the same conditions as those for Fig. 3a.

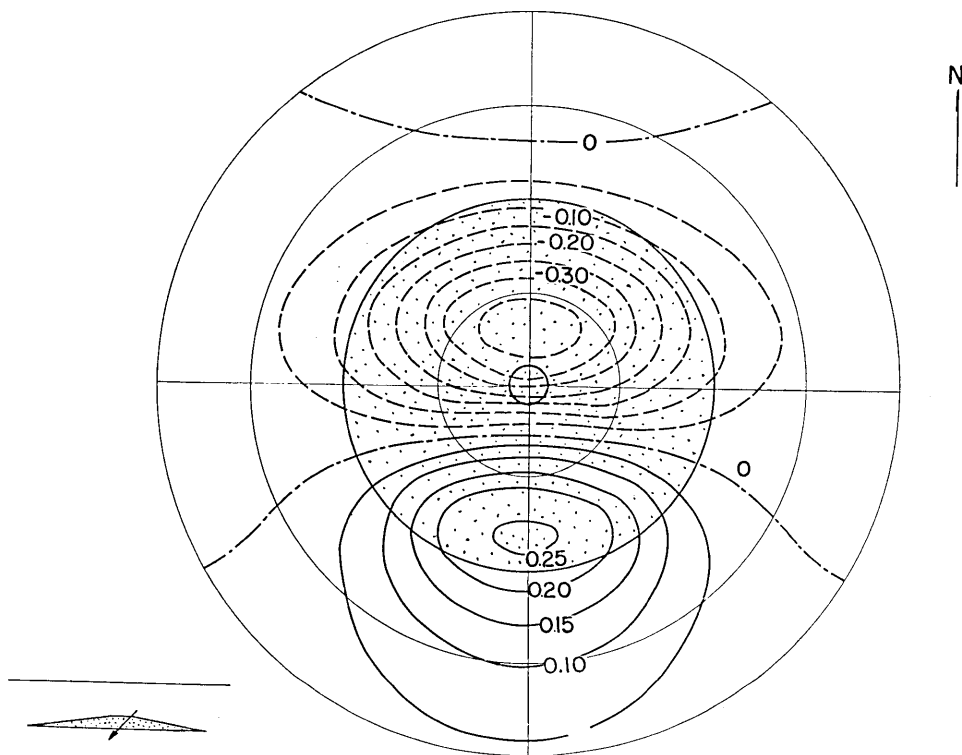


Fig. 4a.  $\Delta X$  over a cone of which all the parameters are the same as those for Fig. 2. The flight height is 0.5.

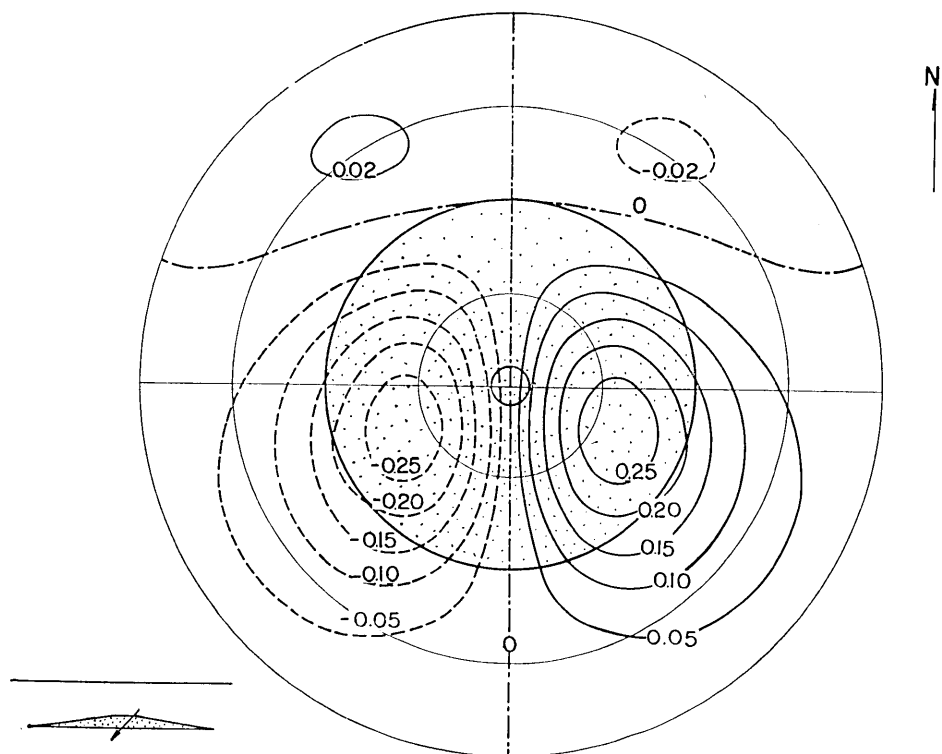


Fig. 4b.  $\Delta Y$  for the same conditions as those for Fig. 4a.

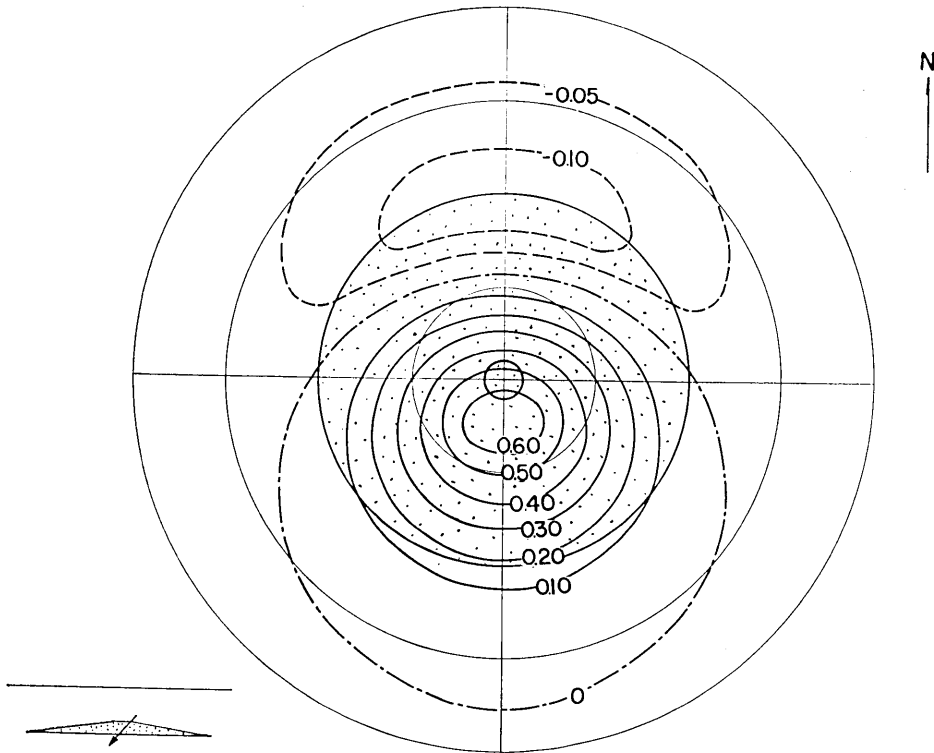


Fig. 4c.  $\Delta Z$  for the same conditions as those for Fig. 4a.

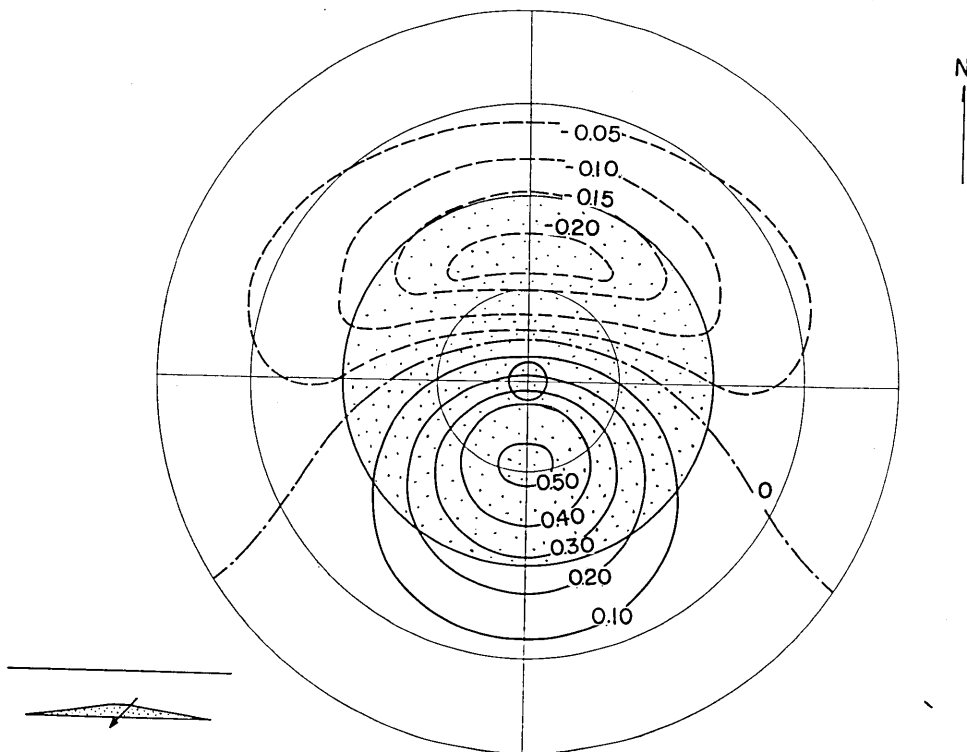


Fig. 4d.  $\Delta F$  for the same conditions as those for Fig. 4a.

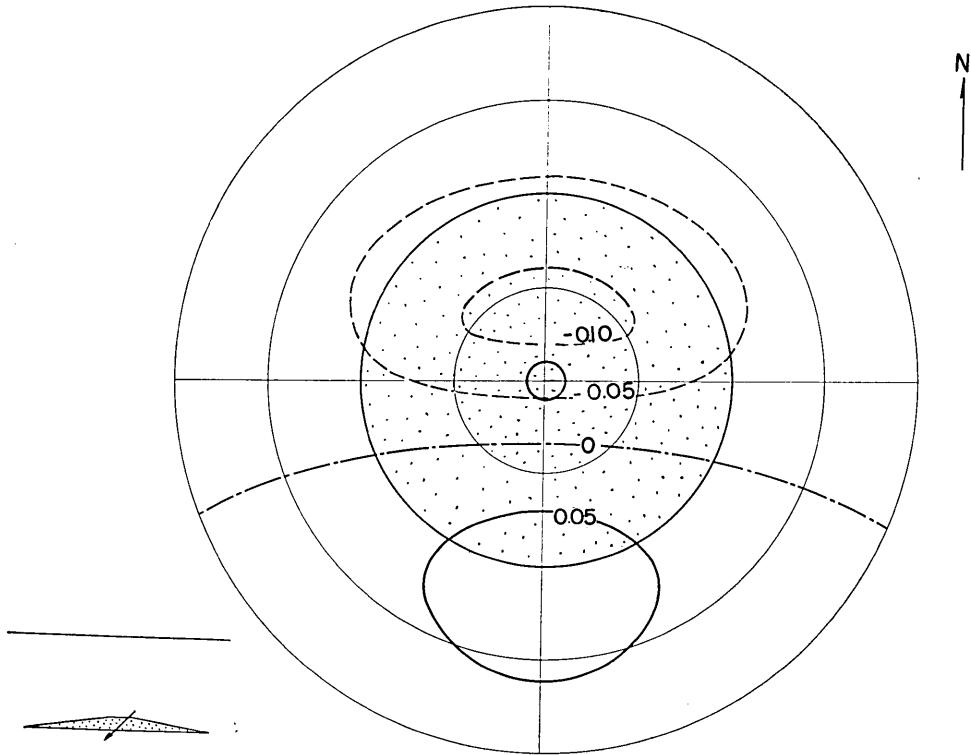


Fig. 5a.  $\Delta X$  over a cone of which all the parameters are the same as those for Fig. 2. The flight height is 1.0.

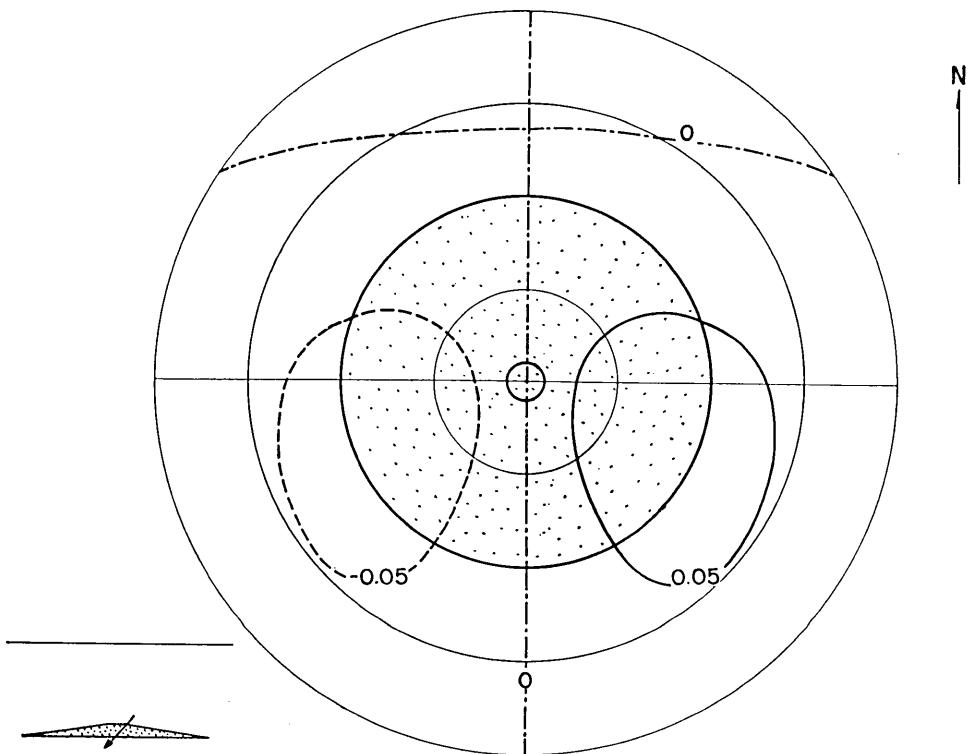


Fig. 5b.  $\Delta Y$  for the same conditions as those for Fig. 5a.

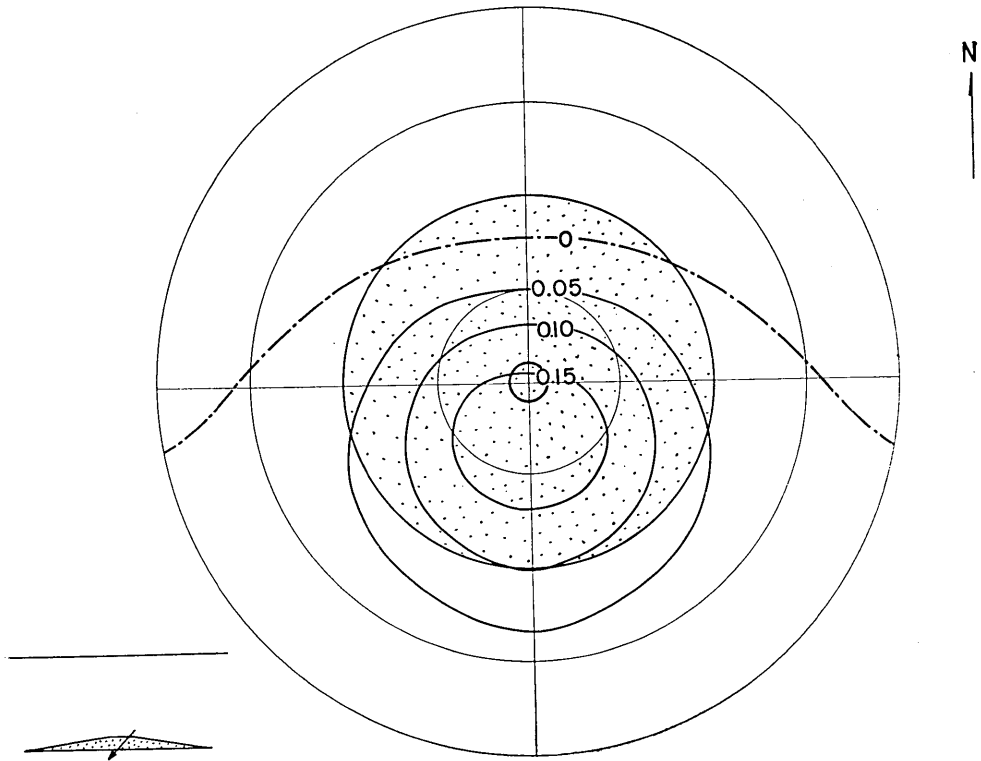


Fig. 5c.  $\Delta Z$  for the same conditions as those for Fig. 5a.

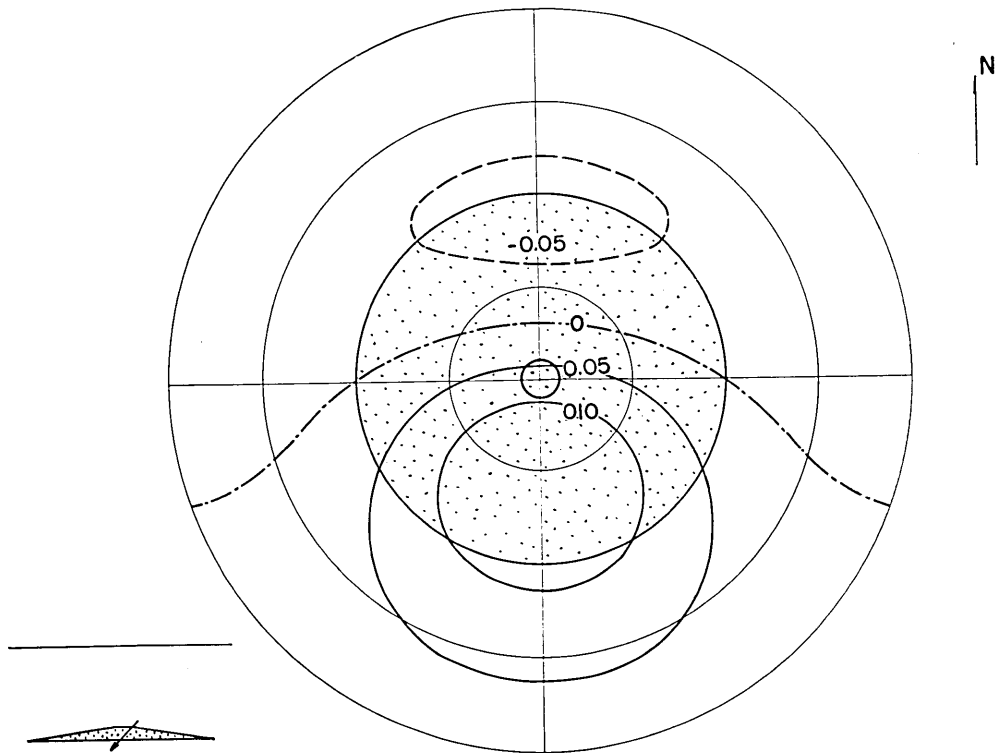


Fig. 5d.  $\Delta F$  for the same conditions as those for Fig. 5a.

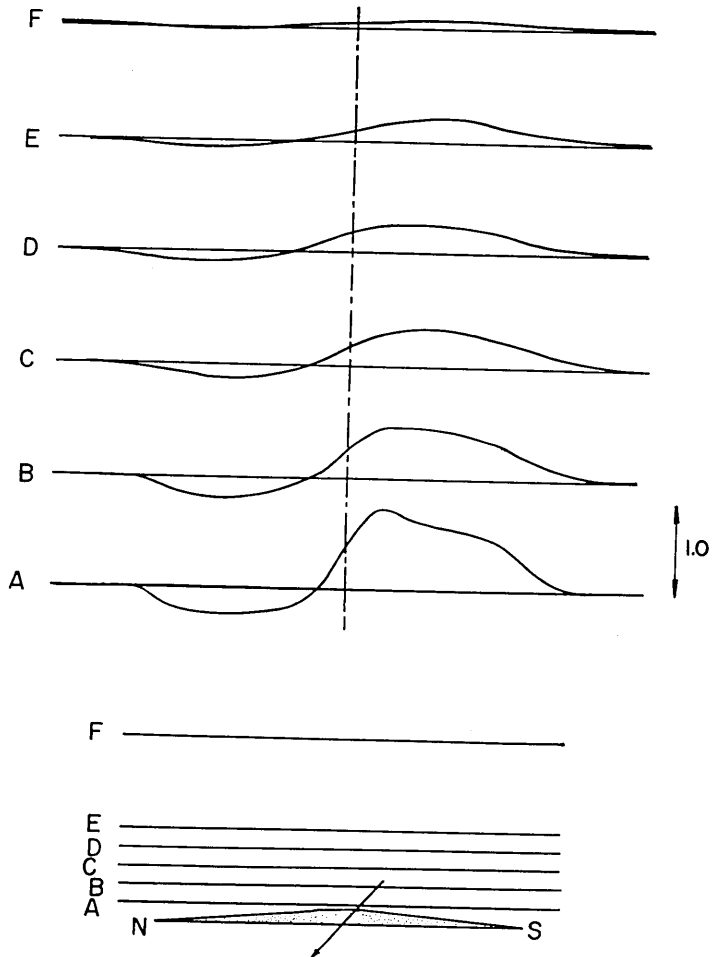


Fig. 6.  $\Delta F$  profiles along the north-south line passing through the centre of a cone of which the slope angle is  $5^\circ$ . The direction of magnetization and its relation to the geomagnetic field have been given in the caption of Fig. 2. The intensity of magnetization and the bottom radius are both taken as unity. The flight heights are taken as 0.1, 0.2, 0.3, 0.4, 0.5 and 1.0.

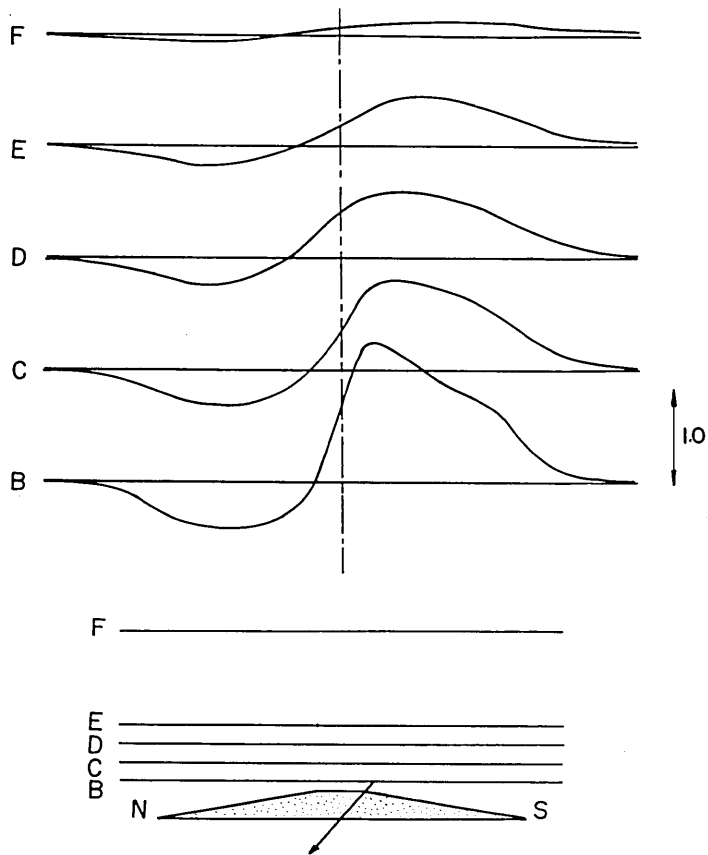


Fig. 7.  $\Delta F$  profiles similar to Fig. 6. The slope angle is  $10^\circ$ . The flight heights are taken as 0.2, 0.3, 0.4, 0.5 and 1.0.

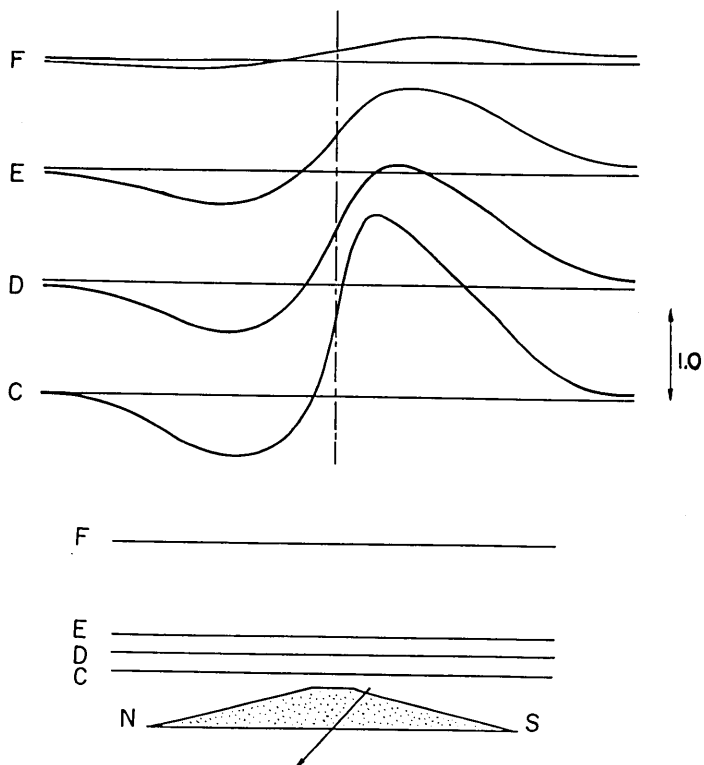


Fig. 8.  $\Delta F$  profiles similar to Fig. 6. The slope angle is  $15^\circ$ . The flight heights are taken as 0.3, 0.4, 0.5 and 1.0.

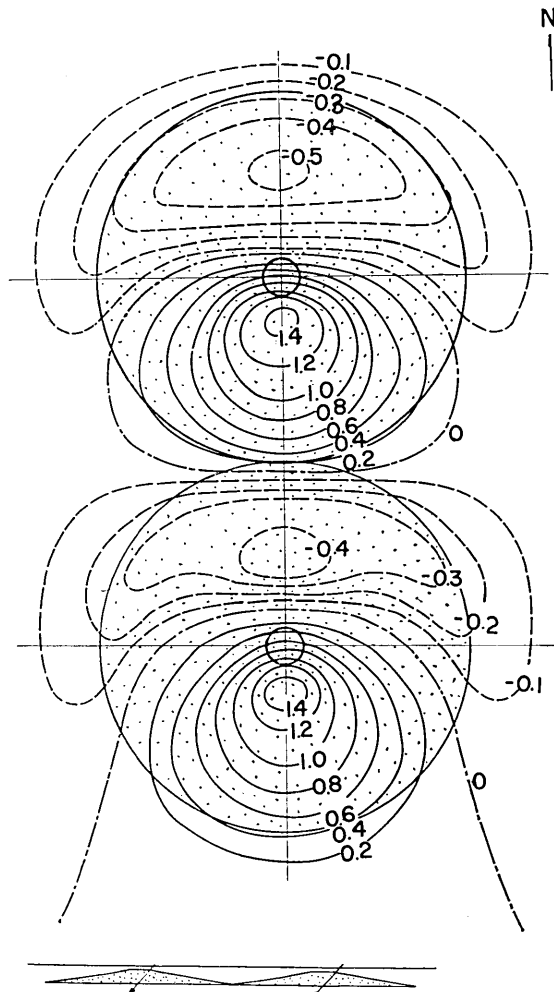


Fig. 9.  $\Delta F$  over two cones closely placed. The line connecting the centres runs in a north-south direction. The parameters of the cones and the relation between the magnetization and the geomagnetic field are the same as those for Fig. 2.

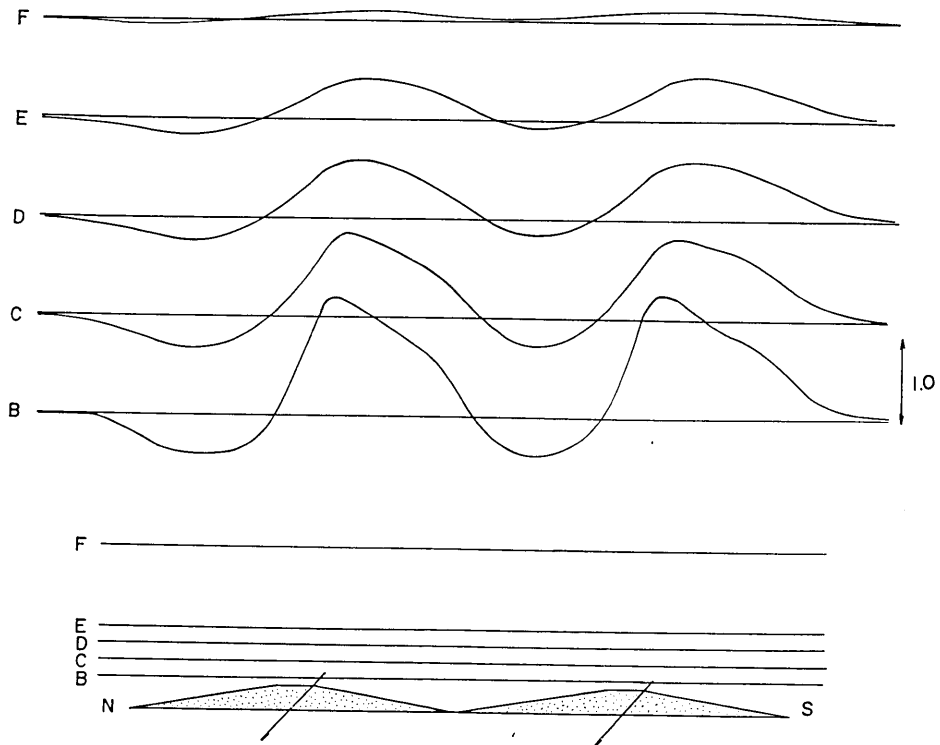


Fig. 10.  $\Delta F$  profiles for the cones as shown in Fig. 10. The flight heights are 0.2, 0.3, 0.4, 0.5 and 1.0.

Profiles of total intensity anomaly along  $x(=x')$  axis are shown in Figs. 6, 7 and 8 respectively for slope angles  $5^\circ$ ,  $10^\circ$  and  $15^\circ$ .

One of the striking features of these profiles is the magnetic high and low respectively towards south and north of the cone.

#### 4. Anomaly over two closely placed cones

The total intensity anomaly over two equivalent cones (slope angle  $10^\circ$ ,  $c_0/a_0=0.1$ ) which are closely placed with one another is calculated. It is assumed that the line connecting the centres of the cones runs in the north-south direction. The purpose of studying such a configuration of magnetized bodies is to examine the magnetic anomaly related to a rugged topography.

Fig. 9 is the anomaly at a height of 0.2, meanwhile Fig. 10 shows

the profiles at various heights along the north-south section through the centres of the cones. If one looks at the anomaly map or profiles without knowing the topography, the magnetic low between the two cones might lead to a conclusion that some weak magnetization or reversed magnetization could possibly be occurring below there. Since the datum value of anomaly is not always clear in aeromagnetic surveys, care should be taken for avoiding such a false conclusion. It is therefore suggested that much attention should be drawn to eliminating the topography effect in investigating underground structure on the basis of an aeromagnetic map.

### 5. Concluding remarks

A computer programme for computing the magnetic effect of a magnetized circular cone was set out. Magnetic anomalies over typical models of volcanoes were then calculated and illustrated. It is confirmed that the anomaly resembles that due to a magnetic dipole. Although nothing quite new has been obtained from the present study, the writers believe that the illustrations of anomaly would be of some use for interpreting aeromagnetic maps. It is also pointed out that topography effect is sometimes serious in the case of an aeromagnetic survey over a mountainous area. The programme could also be used for studying magnetic anomaly associated with a sea mountain.

All the expenses for the computer work in the present paper were defrayed from the Japan Society for the Promotion of Science as part of the Japan-U.S. Cooperative Science Program. The writers are thankful for the support.

### 33. 円錐形帯磁物体に伴なう磁気異常

地震研究所 { 力 武 常 次  
萩 原 幸 男

火山上空の航空磁気測量結果の解釈に應用するために、任意の帯磁をもつ円錐形物体に伴なう磁気異常を計算するプログラムを作り、2, 3 の例を計算した。さらに隣接した 2 個の円錐による磁気異常を調べ、地形の影響により見かけ上 magnetic low があらわれることを指摘した。